Martensitic transformation in Cu-doped NiMnGa magnetic shape memory alloys*

Li Pan-Pan(李盼盼), Wang Jing-Min(王敬民), and Jiang Cheng-Bao(蒋成保)†

Key Laboratory of Aerospace Materials and Performance (Ministry of Education), School of Materials Science and Engineering, Beihang University, Beijing 100191, *China*

(Received 20 August 2010; revised manuscript received 9 September 2010)

This paper studies the martensitic transformation in the Cu-doped NiMnGa alloys. The orthorhombic martensite transforms to $L2_1$ cubic austenite by Cu substituting for Ni in the $Ni_{50-x}Cu_xMn_{31}Ga_{19}$ (x=2–10) alloys, the martensitic transformation temperature decreases significantly with the rate of 40 K per Cu atom addition. The variation of the Fermi sphere radius (k_F) is applied to evaluate the change of the martensitic transformation temperature. The increase of k_F leads to the increase of the martensitic transformation temperature.

Keywords: shape memory alloys, martensitic phase transformation, NiCuMnGa

PACS: 81.30.Kf, 61.66.Dk **DOI:** 10.1088/1674-1056/20/2/028104

1. Introduction

Ferromagnetic shape memory alloys (FSMAs) have drawn lots of attention as a new kind of smart materials for more than one decade.[1−6] Large magnetostrain (magnetic-field-induced strain) of 6%, 9.5% by martensite variants reorientation was achieved in single crystalline NiMnGa ferromagnetic shape memory alloys with 5M and 7M martensite structures,[3−5] and 8.7% magnetostrain was obtained recently in polycrystalline NiMnGa foams.[6] Magnetic field induced reverse martensitic transformation (MFIRMT) was realized in NiCoMnIn FSMAs, companying 3% large magnetic shape memory effect and over 100 MPa output stress.[7] However, due to large anisotropic elasticity modulus, the present FSMAs exhibit intrinsical brittleness. The samples with the large magnetostrain will be broken after several magnetizing circles due to the brittleness, furthermore, we can image that it should be difficult for a brittle sample to export stably large stress up to 100 MPa and large magnetostrain of 3%. This disadvantage limits the practical application of the FSMAs as sensors, actuators, transducers, etc. Therefore, improving the plasticity of FSMAs is a hot topic all the time.

It is inspired that Fe addition in NiMnGa alloy can improve the mechanical properties, especially plasticity.[8,9] And then, the martensitic transformation in the quaternary NiMnFeGa was intensively studied, including magnetostrain, martensitic structure, compositional dependence of phase transformation temperature, and so on.[9−12] Substituting Fe for Mn decreased the martensitic transformation temperature and increased the Curie temperature.[12] Recently, our group found that Cu-doped in NiMnGa could drastically increase the plasticity[13,14] and the MFIRMT was also achieved in the NiMnGaCu alloys.[15] Large magnetostrain, magnetocaloric effect and magnetoresistance are expected in the NiMnGaCu alloys. All these physical effects are based on the martensitic transformation. Here, we focus on the martensitic transformation in NiMnGaCu, revealing the composition dependence of the crystal structure and the martensitic transformation temperature in two series of $Ni_{50-x}Cu_xMn_{31}Ga_{19}$ (x=2–10) and $Ni_{46}Cu_4Mn_{30+y}Ga_{20-y}$ (y=0–6) alloys. The variation of the Fermi sphere radius (k_F) is applied to evaluate the change of the martensitic transformation temperature.

2. Experiments

High-purity elements nickel (99.98%), manganese (99.9%), gallium (99.99%) and copper (99.95%) were

*Project supported by the National Natural Science Foundation for Distinguished Young Scholars of China (Grant No. 50925101), Science Fund for Creative Research Groups of the National Natural Science Foundation of China (Grant No. 50921003) and the Fundamental Research Funds for the Central Universities.

†Corresponding author. E-mail: jiangcb@buaa.edu.cn

© 2011 Chinese Physical Society and IOP Publishing Ltd

polished before use. Ingots of about 30 g were prepared by arc melting and remelted four times. The ingots were annealed at 1173 K for 48 h for homogenization and then quenched in water. Inductively coupled plasma tests confirmed that the actual composition was very close to the nominal composition. The nominal compositions and the corresponding valence electron concentration (e/a) are given in Table 1. Room temperature structure was determined by x-ray diffraction technique using Cu Kα radiation, with powder samples annealed at 773 K for 0.5 h. Phase transformation temperatures higher than room temperature were determined by the differential scanning calorimetry (DSC) (Netzsch STA 449) with the heating/cooling rate of 10 K/min. Temperature dependence of AC susceptibility (χ_{ac}) was measured using a physical properties measurement system (PPMS) to determine transformation temperatures lower than room temperature.

3. Results and discussion

Figure 1 shows the x-ray diffraction patterns taken at room temperature for $Ni_{50-x}Cu_xMn_{31}Ga_{19}$ (x=2–10) and $Ni_{46}Cu_4Mn_{30+y}Ga_{20-y}$ (y=0–6). The lattice parameters and the unit cell volume are calculated according to the diffraction data, as listed in Table 1. For $Ni_{50-x}Cu_xMn_{31}Ga_{19}$ (x=2–10), the phase structure evolves from orthorhombic martensite to cubic austenite with Cu substituting for Ni, as shown in Fig. 1(a). When $x = 2$, the phase structure is orthorhombic martensite, as indicated by the splitting of the (220) peak into (220), (202) and (022) peaks.[16,17] When $x \geq 4$, only the reflections of $L2_1$ austenite phase are observed. The cubic lattice parameter a and the unit cell volume increase from 5.840 Å (1 Å=0.1 nm) and 199.2 Å^3 for $x = 4$ to 5.880 Å and 203.3 Å^3 for $x = 10$, respectively. The increased lattice parameter and unit cell volume are resulted from the larger Cu atoms substitution for Ni atoms.

The room-temperature structure of $Ni_{46}Cu_4Mn_{30+y}Ga_{20-y}$ (y=0–6) alloys evolves from cubic austenite to orthorhombic martensite with Mn substituting for Ga, as shown in Fig. 1(b). When $y = 0$ and 2, reflections of $L2_1$ austenite phase are observed. Diffractions of the orthorhombic martensite are observed when $y \geq 3$. The unit cell volume evolves from 200.4 Å^3 to 196.8 Å^3. The shrinkage of the unit cell is due to the smaller Mn atoms replacing the larger Ga atoms, same as that in $Ni_{50}Mn_{25+x}Ga_{25-x}$ alloys.[17]

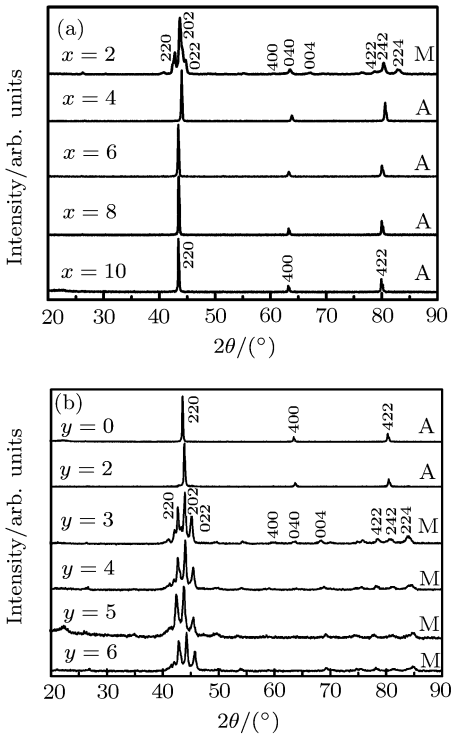


Fig. 1. The x-ray diffraction patterns taken at room temperature for (a) $Ni_{50-x}Cu_xMn_{31}Ga_{19}$ (x=2–10) and (b) $Ni_{46}Cu_4Mn_{30+y}Ga_{20-y}$ (y=0–6) alloys. The abbreviation A represents austenite and M martensite.

Figure 2 representatively shows temperature dependence of the AC susceptibility of $Ni_{44}Cu_6Mn_{31}Ga_{19}$ alloy, and in the inset DSC curve of $Ni_{46}Cu_4Mn_{35}Ga_{15}$ alloy. The sharp changes of the curves are due to the martensitic transformation on cooling and the reverse transformation on heating. The martensite start and finish temperatures M_s and M_f, the austenite start and finish temperatures A_s and A_f, are taken as the temperature where the curve begins to deviate from the baseline, as shown in Fig. 2.

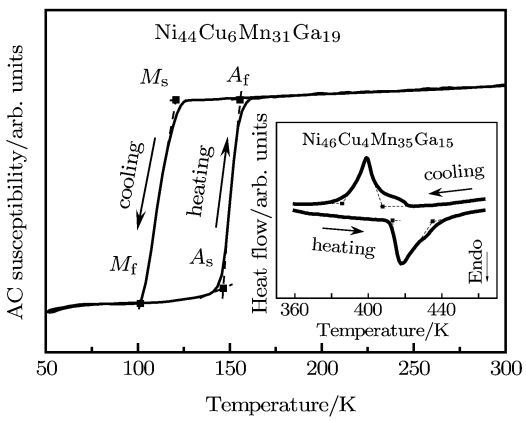


Fig. 2. Temperature dependence of the AC susceptibility (χ_{ac}) measured in the vicinity of the martensitic transformation of $Ni_{44}Cu_6Mn_{31}Ga_{19}$ alloys. Inset shows the DSC curve of $Ni_{46}Cu_4Mn_{35}Ga_{15}$ alloy.

All the measured transformation temperatures for both systems are listed in Table 1.

Figure 3 shows the compositional dependence of the transformation temperatures M_s, M_f, A_s and A_f obtained in (a) $Ni_{50-x}Cu_xMn_{31}Ga_{19}$ (x=2–10) and (b) $Ni_{46}Cu_4Mn_{30+y}Ga_{20-y}$ (y=0–6) alloys, including $Ni_{48}Cu_2Mn_{31}Ga_{19}$ and $Ni_{46}Cu_4Mn_{31}Ga_{19}$, as reported previously.[18] There are quite different variations in the transformation temperatures versus composition in the two systems. For $Ni_{50-x}Cu_xMn_{31}Ga_{19}$ alloys, M_s is significantly decreased by substituting Cu for Ni, with the average decrease rate of 40 K per Cu atom addition. There is no martensitic transformation found in $Ni_{42}Cu_8Mn_{31}Ga_{19}$ and $Ni_{40}Cu_{10}Mn_{31}Ga_{19}$ alloys. For $Ni_{46}Cu_4Mn_{30+y}Ga_{20-y}$ alloys, the transformation is obviously shifted to higher temperature range, with the average M_s increasing rate of 50 K per Mn atom substituting for Ga. The decreasing rate of M_s caused by Mn replacing Ga in the present $Ni_{46}Cu_4Mn_{30+y}Ga_{20-y}$ system is much higher than 30 K in previously reported $Ni_{50}Mn_{25+x}Ga_{25-x}$ alloys.[17] Therefore, Cu addition raises the sensitivity of transformation temperatures to the composition. Besides, the transformation hysteresis, A_f–M_s, is broadened in $Ni_{50-x}Cu_xMn_{31}Ga_{19}$ systems by doping Cu. The increased compositional sensitivity and the broadened hysteresis in NiCuMnGa alloys are contrary to NiTiCu shape memory alloys, where the compositional sensitivity is weakened and the hysteresis is narrowed by substituting Cu for Ni.[19]

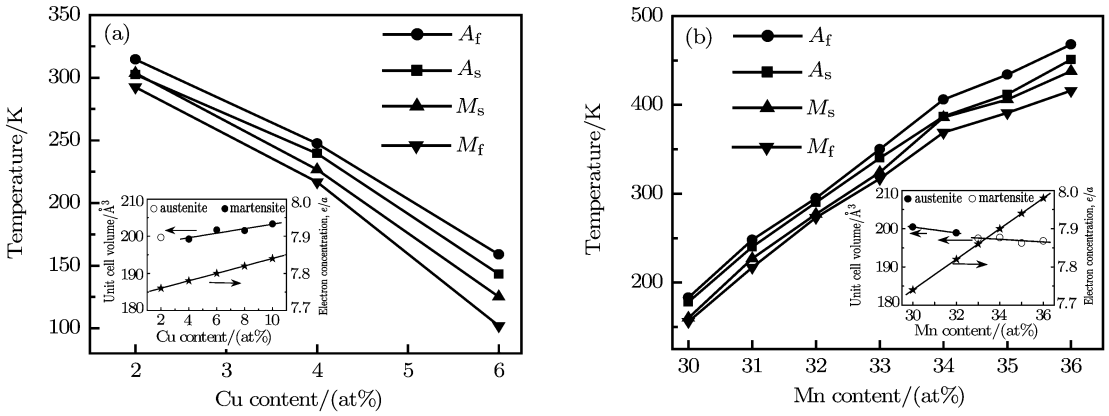


Fig. 3. The compositional dependence of the transformation temperatures M_s, M_f, A_s and A_f of (a) $Ni_{50-x}Cu_xMn_{31}Ga_{19}$ (x=2–6) alloys and (b) $Ni_{46}Cu_4Mn_{30+y}Ga_{20-y}$ (y=0–6) alloys. Insets show the variation of the unit cell volume and the electron concentration of both systems, respectively.

Based on the Hume–Rothery mechanism, the size factor and the valence electron concentrations as two important parameters are considered to influence the transformation temperatures.[20] It has been reported that smaller unit cell volume and higher electron concentration could increase the martensitic transformation temperatures.[20] In the present work, for $Ni_{50-x}Cu_xMn_{31}Ga_{19}$ (x=2–10) alloys, the unit cell volume is enlarged by substituting Cu for Ni, which results in the decrease of the martensitic transformation temperatures. And for $Ni_{46}Cu_4Mn_{30+y}Ga_{20-y}$ (y=0–6) alloys, substituting Mn for Ga results in severe shrinkage of the unit cell, which contributes to the increased transformation temperatures. This matches well with the Hume–Rothery mechanism and is in good agreement with the conclusion that has been proved in many FSMAs.[17,21]

For the $Ni_{46}Cu_4Mn_{30+y}Ga_{20-y}$ (y=0–6) alloys, the increase of the electron concentration by substituting Mn ($3d^54s^2$) for Ga ($4s^24p^1$) results in the increase of the transformation temperatures. This is also consistent with the previous results in other FSMAs.[17,21] However, for the $Ni_{50-x}Cu_xMn_{31}Ga_{19}$ (x=2–10) alloys, the electron concentration is increased by substituting Cu ($3d^{10}4s^1$) for Ni ($3d^84s^2$), the martensitic transformation temperatures decrease, this fact is contrary to the previous reports.

When the Fermi sphere is tangent to or smaller than the first Brillouin zone, the phase structure is stable. And when the electrons are above the Fermi level, they move to the corner states of the first Brillouin zone, and the excessive increase of energy of system results in the distortion of the lattice to minimize the free energy, which should lead to the martensitic transformation.[21] Here we use the variation of the Fermi sphere radius (k_F) to evaluate the change

of the martensitic transformation temperature. The Fermi sphere radius ($k_{\rm F}$) can be preliminarily estimated as[22]

$$k_F = 2\pi \left(\frac{3}{8\pi}\right)^{1/3} \left(\frac{N}{V}\right)^{1/3}, \qquad (1)$$

where N is the valence electron concentration per unit cell, V is the unit cell volume. It is calculated that the $k_{\rm F}$ decrease from 2.641 Å^{-1} for $x = 2$ to 2.634 Å^{-1} for $x = 10$ in $Ni_{50-x}Cu_xMn_{31}Ga_{19}$ alloys. The decrease of $k_{\rm F}$ means that the parent phase is more stable. Thus, the decrease of $k_{\rm F}$ leads to the decrease of the martensitic transformation temperatures in the $Ni_{50-x}Cu_xMn_{31}Ga_{19}$ alloys. For $Ni_{46}Cu_4Mn_{30+y}Ga_{20-y}$ (y=0–6) alloys, the $k_{\rm F}$ increases from 2.635 Å^{-1} for $y = 0$ to 2.678 Å^{-1} for $y = 6$. The increase of $k_{\rm F}$ results in the increase of the martensitic transformation temperatures.

Table 1. Room-temperature crystal structures, lattice parameters, unit-cell volumes, transformation temperatures and hysteresis, and electronic concentrations (e/a) of $Ni_{50-x}Cu_xMn_{31}Ga_{19}$ (x=2–10) and $Ni_{46}Cu_4Mn_{30+y}Ga_{20-y}$ (y=0–6) alloys.

alloys	room-temperature crystal structure	lattice parameters			unit cell	transformation temperatures/K				hysteresis	e/a
		a/Å	b/Å	c/Å	volume/Å^3	$A_{\rm s}$	$A_{\rm f}$	$M_{\rm s}$	$M_{\rm f}$	$(A_{\rm f}-M_{\rm s})$/K	
x=2	orthorhombic	6.111	5.859	5.576	199.6	303	315	304	293	11	7.76
x=4	$L2_1$	5.840	5.840	5.840	199.2	240	248	227	217	21	7.78
x=6	$L2_1$	5.865	5.865	5.865	201.7	143	159	125	102	34	7.80
x=8	$L2_1$	5.863	5.863	5.863	201.5	–	–	–	–	–	7.82
x=10	$L2_1$	5.880	5.880	5.880	203.3	–	–	–	–	–	7.84
y=0	$L2_1$	5.852	5.852	5.852	200.4	178	183	160	156	23	7.74
y=2	$L2_1$	5.837	5.837	5.837	198.9	290	295	277	273	18	7.82
y=3	orthorhombic	6.136	5.847	5.504	197.5	340	350	324	317	26	7.86
y=4	orthorhombic	6.231	5.821	5.451	197.7	387	406	386	369	20	7.90
y=5	orthorhombic	6.261	5.786	5.418	196.3	412	434	406	391	28	7.94
y=6	orthorhombic	6.239	5.826	5.416	196.8	451	468	438	416	30	7.98

4. Conclusion

In summary, the orthorhombic martensite transforms to $L2_1$ cubic austenite at ambient temperature by substituting Cu for Ni in the $Ni_{50-x}Cu_xMn_{31}Ga_{19}$ (x=2–10) alloys, the martensitic transformation temperature is significantly decreased. The Cu addition in $Ni_{46}Cu_4Mn_{30+y}Ga_{20-y}$ (y=0–6) alloys enhance the sensitivity of the transformation temperatures dependent on the Mn content. The variation of the Fermi sphere radius ($k_{\rm F}$) is applied to evaluate the change of the martensitic transformation temperature. The increase of $k_{\rm F}$ leads to the increase of the martensitic transformation temperature.

References

[1] Ullakko K, Huang J K, Kantner C, O'Handley R C and Kokorin V V 1996 *Appl. Phys. Lett.* **69** 1966

[2] Meng F B, Guo H J, Liu G D, Liu H Y, Dai X F, Luo H Z, Li Y X, Chen J L and Wu G H 2009 *Chin. Phys.* B **18** 3031

[3] Murray S J, Marioni M, Allen S M, O'Handley R C and Lograsso T A 2000 *Appl. Phys. Lett.* **77** 886

[4] Sozinov A, Likhachev A A, Lanska N and Ullakko K 2002 *Appl. Phys. Lett.* **80** 1746

[5] Cui Y T, You S Q, Wu L, Ma Y, Chen J L, Pan F S and Wu G H 2009 *Acta Phys. Sin.* **58** 8596 (in Chinese)

[6] Chmielus M, Zhang X X, Witherspoon C, Dunand D C and Müllner P 2009 *Nature Mater.* **8** 863

[7] Kainuma R, Imano Y, Ito W, Sutou Y, Morito H, Okamoto S, Kitakami O, Oikawa K, Fujita A, Kanomata T and Ishida K 2006 *Nature* (London) **439** 957

[8] Cherechukin A A, Dikshtein I E, Ermakov D I, Glebov A V, Koledov V V, Kosolapov D A, Shavrov V G, Tulaikova A A, Krasnoperov E P and Takagi T 2001 *Phys. Lett.* A **291** 175

[9] Wan J F, Fei Y Q and Wang J N 2006 *Acta Phys. Sin.* **55** 2444 (in Chinese)

[10] Liu Z H, Chen J L, Hu H N, Zhang M, Dai X F, Zhu Z Y, Liu G D, Wu G H, Meng F B and Li Y X 2004 *Scripta Mater.* **51** 1011

[11] Wang H B, Sui J H, Liu C and Cai W 2008 *Mater. Sci. Eng.* A **480** 472

[12] Mathur R P, Singh R K, Chandrasekaran V, Ray S and Ghosal P 2007 *Metall. Mater. Trans.* A **38** 2076

[13] Wang J M, Bai H Y, Jiang C B, Li Y and Xu H B 2010 *Mater. Sci. Eng.* A **527** 1975

[14] Wang J M and Jiang C B 2010 *Scripta Mater.* **62** 298

[15] Li P P, Wang J M, Jiang C B and Xu H B *Appl. Phys. Lett.* submitted

[16] Wang W H, Liu Z H, Zhang J, Chen J L, Wu G H, Zhan W S, Chin T S, Wen G H and Zhang X X 2002 *Phys. Rev.* B **66** 052411

[17] Jiang C B, Muhammad Y, Deng L F, Wu W and Xu H B 2004 *Acta Mater.* **52** 2779

[18] Jiang C B, Wang J M, Li P P, Jia A and Xu H B 2009 *Appl. Phys. Lett.* **95** 012501

[19] Grossmann Ch, Frenzel J, Sampath V, Depka T and Eggeler G 2009 *Metall. Mater. Trans.* A **40** 2530

[20] Chernenko V A 1999 *Scripta Mater.* **40** 523

[21] Jiang C B, Feng G, Gong S K and Xu H B 2003 *Mater. Sci. Eng.* A **342** 231

[22] Huang K and Han N Q 1988 *Solid State Physics* Vol. 1 (Beijing: Higher Education Press) p. 220 (in Chinese)